Observation of high-*Q* optomechanical modes in the mounted silica microspheres

Zhen Shen,[1,2] Zhong-Hao Zhou,[1,2] Chang-Ling Zou,[1,2] Fang-Wen Sun,[1,2] Guo-Ping Guo,[1,2] Chun-Hua Dong,[1,2,*] and Guang-Can Guo[1,2]

[1]*Key Laboratory of Quantum Information, Chinese Academy of Sciences, University of Science and Technology of China, Hefei 230026, China*

[2]*Synergetic Innovation Center of Quantum Information and Quantum Physics, University of Science and Technology of China, Hefei, Anhui 230026, China*

**Corresponding author: chunhua@ustc.edu.cn*

Received June 24, 2015; revised July 30, 2015; accepted July 30, 2015; posted August 3, 2015 (Doc. ID 243647); published August 24, 2015

An efficient method to mount a coupled silica microsphere and tapered fiber system is proposed and demonstrated experimentally. For the purpose of optomechanical studies, high-quality-factor optical ($Q_o \sim 10^8$) and mechanical modes ($Q_m \sim 0.87 \times 10^4$) are maintained after the mounting process. For the mounted microsphere, the coupling system is more stable and compact and, thus, is beneficial for future studies and applications based on optomechanical interactions. Especially, the packaged optomechanical system, which is tested in a vacuum chamber, paves the way toward quantum optomechanics research in cryostat.

OCIS codes: (230.5750) Resonators; (230.3990) Micro-optical devices; (120.4880) Optomechanics.
http://dx.doi.org/10.1364/PRJ.3.000243

1. INTRODUCTION

In the past decade, cavity optomechanics has been extensively studied in a variety of macro-, micro-, and nano-optical systems [1,2]. A number of remarkable optomechanical phenomena have been reported in experiments, ranging from amplifying and cooling of phonon modes [3–6], optomechanically induced transparency [7–9], and strong coupling between mechanical oscillator and optical cavity [10] to various mechanical applications [8–20]. Among these systems, whispering gallery mode (WGM) microresonators [21–23] have attracted a lot of attention due to their ease of fabrication, ultrahigh optical *Q*-factor, and various high-*Q* mechanical vibration modes.

However, the material absorption limited high-*Q* optical WGMs can only be excited efficiently through near field couplers [24] such as a silica fiber taper. Stable 3D optical stages are required to hold the microresonator-taper coupling system to keep and adjust the air gap between them and, thus, give rise to experiment difficulties in a relatively small vacuum chamber or cryostat [25]. To address this issue, several mounted methods have been proposed, and the high-*Q* WGM microresonators for practical sensing, filter applications, or microlasing are demonstrated [26–31]. Because we are typically concerned with the optical properties of the WGMs, the properties of the mechanical vibration of these microresonators have been overlooked in previous package schemes. For example, extra-polymer glue or the fiber taper adhered to the microresonator will significantly destroy the mechanical *Q*.

In this paper, we present the mounted microsphere system maintaining high optical and mechanical *Q* factor without further adjustments. Our experiments demonstrate how to maintain high optical and mechanical *Q*-factors when the tapered fiber is contacted to the microsphere. Other advantages of this packaging system includes simple operation to package, long time stabilization in ambient, even in a vacuum chamber. In addition, the packaged framework is made by the same material silica, thus the whole system is insensitive to temperature changes. Therefore, we believe that our packaged system is promising for future experiments in the cryostat without a 3D translation stage, thus avoiding the complicated imaging system [25].

A. Experiment Setup and Package

Figure 1(a) shows a schematic of the experimental setup. The silica microspheres (diameter about 50 μm) were fabricated by melting the tapered tip of a fiber through a continuous wave (CW) CO_2 laser. Generally, the higher mechanical *Q* factor could be obtained with the appropriate size of the stem [32] and the symmetry structure [33]. As shown in the inset of Fig. 1(a), the mechanical *Q* factor of the microsphere is near 10^4 with the stem diameter of 7 μm and stem length of 40 μm. The tapered fiber for evanescently coupling was obtained by melting a standard SMF-28 silica optical fiber with a hydrogen flame.

The packaging procedure consists of three steps, which are shown in Figs. 1(b)–1(d). The first step is to fix the acrylate buffer of the glass stem, which supports the microsphere to the center shaft of the C-shape glass plate by a UV glue. After that, the microsphere is fixed to the package framework. Then, a fiber taper is moved to the vicinity of the microspheres by a 3D translation stage. The relative position and distance related to the microsphere are precisely adjusted. During this step, the optical spectrum is monitored simultaneously to ensure an efficient coupling between the fiber taper and optical WGMs. In the last step, the tapered fiber is transferred from

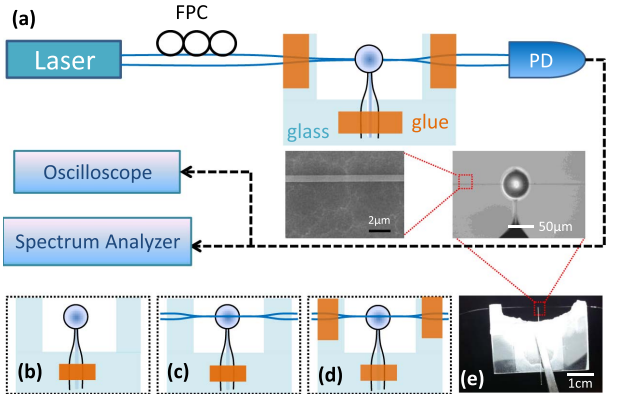

Fig. 1. (a) Experimental setup for the packaged microsphere. FPC, fiber polarization controller; PD, photodetector. (b)–(d) Illustration of the packaging process. (e) Typical packaged microsphere-taper coupling system. (Inset) SEM images of tapered fiber and digital image of the coupled silica microsphere and tapered fiber system.

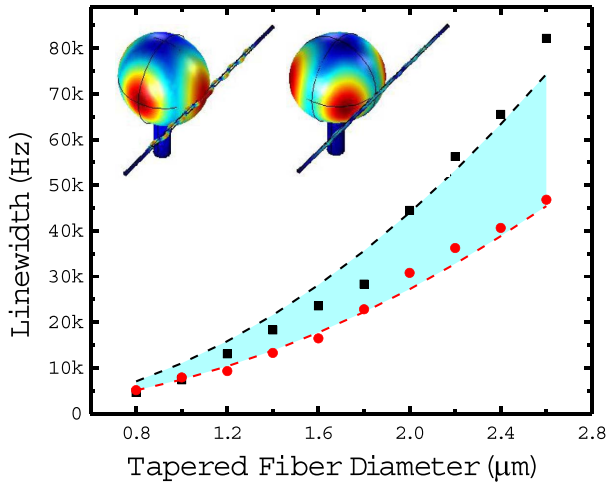

Fig. 2. Numerical simulated mechanical dissipation due to fiber taper touched with the microsphere. Black and red dots correspond to two mechanical modes with lifted degeneracy due to taper fiber, as shown by the two inset figures. Dashed lines are fitting results.

the homemade stage to the glass stage by the UV glue, as shown in Fig. 1(d). The whole system is also monitored in real-time through a CCD camera during the processes of packaging, as shown in the inset of Fig. 1(a). Figure 1(e) shows one typical packaged microsphere.

Following the aforementioned procedures, packaged microsphere-fiber taper systems are characterized by the setup shown in Fig. 1(a). To observe the mechanical vibrations, the tunable diode laser (1550 or 780 nm) is launched into the tapered fiber and coupled into the microspheres through an evanescent field. When the probe laser is slightly detuned from the cavity resonator, the thermal displacement of the mechanical resonator is transduced to the optical signal as amplitude-modulated radio-frequency signals. Note that the power of the probe laser should be low enough to avoid thermal [34], Kerr [35] or optomechanical instability [36]. The output light from the tapered fiber is sent to a detector, which is connected to an electronic spectrum analyzer and a digital oscilloscope. Then, the optical transmission spectrum and the power spectrum of the mechanical vibrations are obtained. A paddle fiber polarization controller (FPC) is used to change the polarization state of the input laser.

After mounting, the optical and mechanical Q factor can be kept similar as before, as will be discussed later in this text. Moreover, as the packaged system is made of essentially the same glass material, the tapered fiber will remain synchronously thermal contraction as temperature changes. Thus, we believe that the mounted microsphere and taper fiber system can be applied in the cryostat [37]. During the experiment, the glass plate with microsphere was risen up from underneath of the tapered fiber until mutual touching. The glass plate should be strictly parallel to the tapered fiber. Otherwise, one side of the glass plate would first come into contact with the tapered fiber but not the microsphere. In addition, during the touching process, the microsphere could not be drastically raised up. In other words, the tapered fiber with high tension would slip away from the equator of the microsphere.

B. Results

1. Numerical Investigation

Before the experiments, we numerically investigated the mechanical dissipation of the microsphere due to the tapered fiber touching by using the finite-element method solver (COMSOL Multiphysics v4.2). The diameters of the microsphere and its stem were fixed to be 50 μm and 10 μm, respectively. The calculated mechanical dissipation rate of the S21 modes for the diameter of the tapered fiber varied from 0.8 μm to 2.6 μm are shown in Fig. 2. If the microcavity is untouched with tapered fiber, there are two degenerated mechanical modes, with frequency around 63 MHz and mechanical dissipation rate smaller than 100 Hz. Note that, in our calculation, only external radiation (clamping) losses due to tapered fiber and stems are considered, and we know the mechanical dissipation rate should be around 1.2 kHz at room temperature [38]. When tapered fiber is touching with the sphere, the dissipation rate significantly increased. An intuitive understanding is that the acoustic energy leakage by the tapered fiber is proportional to the area of the fiber. Therefore, we fitted the losses that quadratically increase with the tapered fiber diameter, which are shown by the dashed lines in Fig. 2. The two sets of data correspond to the degenerated S21 modes: one is coupling to the tapered fiber with maximum displacement; the other is coupling to the tapered fiber by the node. Therefore, the mechanical dissipation rate is lower for the later mechanical mode. In practical experiments, the imperfection sphere geometry will also induce the degeneracy of S21 modes; therefore, we can expect that the touched tapered-fiber-induced loss fall in the region between two dashed lines (the shadow area in Fig. 2).

2. Characterization by NIR Light

To demonstrate the package and verify the effect of tapered fiber touching, we first carried out the experiment at 1550 nm wavelength. Figure 3(a) shows the mechanical linewidth of three different microspheres against the diameter of tapered fiber before and after the touching. The behavior is remarkably reproducible for the different samples. Comparing the linewidth to the untouched microsphere, the increment of the linewidth is about 2 kHz for taper diameter is 800 nm, which agrees well with our simulation results. For a larger diameter of touching fiber tapers, we observed that the linewidth of the sample mechanical mode increases quadratically,

which is consistent with the prediction in Fig. 2. Figures 3(b) and 3(c) show typical power spectrum of the mechanical vibration of sample A with a tapered diameter around 800 nm. The mechanical Q factor degraded to 8770 after touching as compared with 9730 before touching. For other positions, the mechanical Q factor spoiled obviously close to three times.

The mechanisms of intrinsic mechanical dissipation of the microsphere include clamping losses, viscous damping, and materials-induced losses [1,38]. The clamping losses, which are determined by the structure of the supports of the oscillator, especially the ratio between the diameter of the microsphere and its stem in our case, dominate the limit of the mechanical quality of our devices. In addition, the viscous damping, which is caused by interactions with the surrounding gas atoms in our experiment, is almost constant for different spheres and can be fully eliminated in a vacuum chamber ($p < 1$ mbar). Therefore, due to the slightly different geometry of the spheres, the three samples have different mechanical dissipation rates and show different changes of dissipation rate for the same fiber taper size.

It is worth noting that the touched optical Q factors drop drastically when the coupling position is good for the touched mechanical Q, as shown in Figs. 3(d) and 3(e). As we know, the optical coupling rate between the microsphere and the tapered fiber are determined by the evanescent fields overlap and phase matching conditions [39]. For the given wavelength laser, the touched optical Q could be kept high at the appropriate position [26]. Otherwise, the optical Q is spoiled quickly. As previously discussed, the touched mechanical Q could be kept with the tapered fiber diameter of 800 nm. For such size of tapered fiber, the touched optical Q factors could be kept with short wavelength [40]. In order to simultaneously obtain high optical and mechanical Q factors, we run the experiment using the visible light.

3. Characterization by Visible Light

In order to circumvent the dramatic decline of the optical modes, we changed the setup to 780 nm wavelength. The waist of typical 780 nm monomode tapered fiber is approximately 800 nm [41], which should slightly spoil the mechanical Q_m. Figure 4(a) shows the touched mechanical Q_m factor for different positions on the taper while the contact point is on the equator of the sphere. The interval between different positions is roughly 100 μm for the tapered fiber with a diameter of 800 nm, as shown in the SEM image in Fig. 1(a).

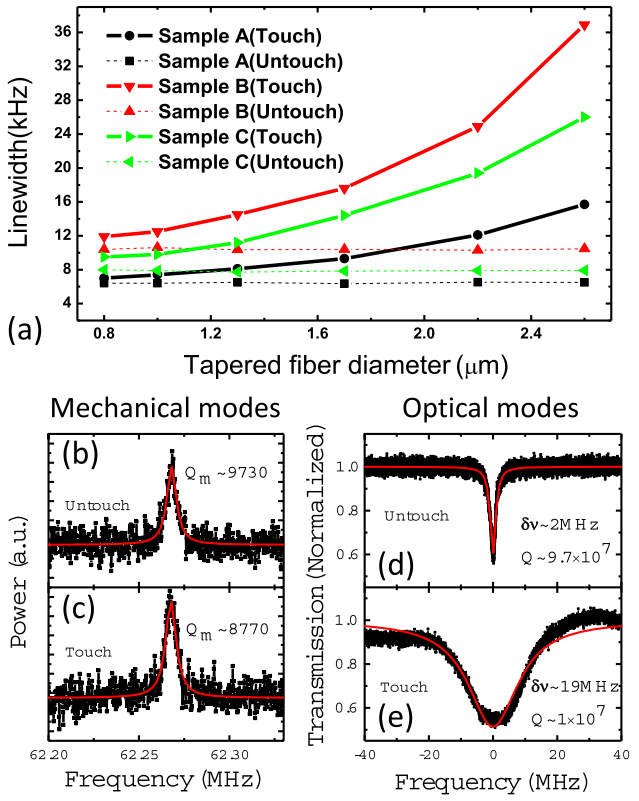

Fig. 3. (a) Mechanical linewidth versus the tapered fiber diameter for three different samples before and after the touching, respectively. (b) and (c) Power spectrum of the mechanical vibrations before and after the touching for sample A, the position of which the tapered fiber diameter is about 800 nm. (d) and (e) Transmission spectrum of sample A before and after the touching at the same position as (b) and (c). These results were obtained under 1550 nm wavelength laser. Mechanical frequencies of the three samples are $\omega_m/2\pi \approx 62.2$ MHz, 59.3 MHz, 57.6 MHz, respectively.

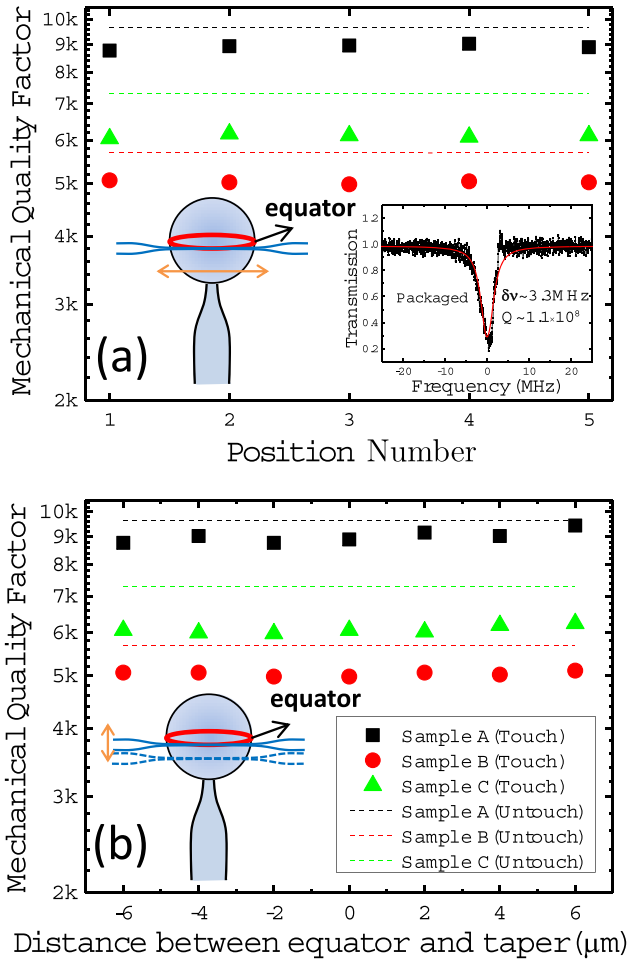

Fig. 4. (a) Touched mechanical Q factor of three samples at five positions in which the interval is roughly 100 μm of a typical 780 nm single-mode tapered fiber, respectively. (b) Mechanical Q factor of three samples versus the perpendicular distance between the equator of the microsphere and the tapered fiber. (Inset) Touched transmission spectrum of sample A excited by 780 nm laser. Dashed lines indicate untouched mechanical Q factor for guiding.

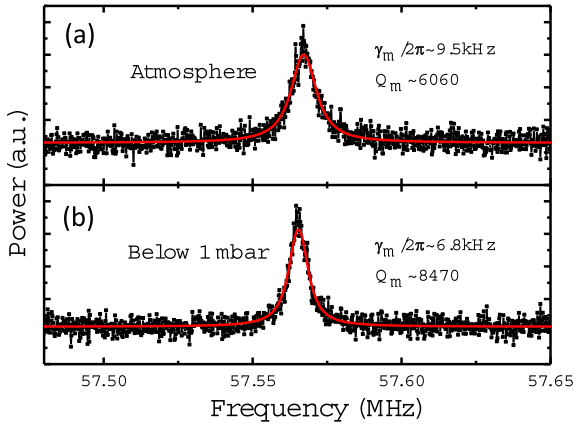

Fig. 5. (a) and (b) Power spectrum of the mechanical vibrations in atmospheric pressure and in a vacuum for the packaged microresonator system, respectively.

We also studied the touched mechanical Q_m with different positions along the polar direction on the microsphere, as shown in Fig. 4(b). All results indicate that the Q_m is insensitive to the contact points. During this process, the high optical modes can be observed all the time. A typical transmission spectrum of sample A indicates the Q factor up to 10^8 [inset of Fig. 4(a)]. The asymmetric lineshape in the tail of the transmission shows the ringing phenomenon [42]. The higher Q factor of the optical mode would pull the system in the resolved band regime and greatly decrease the threshold for the pump power [$P \propto 1/Q_o^3$], which is good for the application of cavity optomechanics. These results indicate that, even without the high-resolution 3D translation stage, high mechanical and optical Q factors can be obtained after the packaging process. Moreover, we could infer that, even in the encapsulation process, the micrometer order of magnitude change of the relative position, the mechanical quality would not be affected.

To verify the practicability of the mounted scheme, experiments in vacuum were also carried out. Figures 5(a) and 5(b) are the power spectrum of mechanical vibration in atmospheric pressure and in vacuum for one mounted system. It is found that the mechanical Q factor is even higher than the results in air before the package because of the absent air damping. The process of measurement was extremely simple without the 3D translation stage. We simply needed to carefully put the glass plate into the vacuum cavity.

2. CONCLUSIONS

In conclusion, we propose a method to mount a silica microsphere-fiber coupling system for optomechanical study. We pay close attention to maintain a high mechanical Q factor and simultaneously to maintain an ultrahigh optical Q factor. In the experiment, we discover that the mounted coupling system, which is operated on a 780 nm wavelength, can achieve this goal because 780 nm wavelength can match up well with the waist size of the tapered fiber, which is small enough to reduce the mechanical clamping losses. The experiment in a vacuum is also carried out to verify the practicability of the packaged system. The result shows that the touched mechanical Q factor can be improved without the air damping. This work will not only make the experiments on microcavity optomechanics convenient and low cost in a vacuum and cryostat but pave the way to the sensing and quantum information applications of cavity optomechanical oscillation.

ACKNOWLEDGMENT

The work was supported by the Strategic Priority Research Program(B) of the Chinese Academy of Sciences (grant no. XDB01030200), National Basic Research Program of China (grant nos. 2011CB921200 and 2011CBA00200) and the National Natural Science Foundation of China (grant no. 61308079), and Anhui Provincial Natural Science Foundation (grant no. 1508085QA08), the Fundamental Research Funds for the Central Universities.

REFERENCES

1. T. J. Kippenberg and K. J. Vahala, "Cavity optomechanics: back-action at the mesoscale," Science **321**, 1172–1176 (2008).
2. M. Aspelmeyer, T. J. Kippenberg, and F. Marquardt, "Cavity optomechanics," Rev. Mod. Phys. **86**, 1391–1452 (2014).
3. A. Schliesser, R. Rivière, G. Anetsberger, O. Arcizer, and T. J. Kippenberg, "Resolved-sideband cooling of a micromechanical oscillator," Nat. Phys. **4**, 415–419 (2008).
4. A. Schliesser, O. Arcizer, R. Rivière, G. Anetsberger, and T. J. Kippenberg, "Resolved-sideband cooling and position measurement of a micromechanical oscillator close to the Heisenberg uncertainty limit," Nat. Phys. **5**, 509–514 (2009).
5. Y.-S. Park and H. Wang, "Resolved-sideband and cryogenic cooling of an optomechanical resonator," Nat. Phys. **5**, 489–493 (2009).
6. J. Chan, T. P. Mayer Alegre, A. H. Safavi-Naeini, J. T. Hill, A. Krause, S. Gröblacher, M. Aspelmeyer, and O. Painter, "Laser cooling of a nanomechanical oscillator into its quantum ground state," Nature **478**, 89–92 (2011).
7. S. Weis, R. Rivière, S. Deléglise, E. Gavartin, O. Arcizet, A. Schliesser, and T. J. Kippenberg, "Optomechanically induced transparency," Science **330**, 1520–1523 (2010).
8. H. Safavi-Naeini, T. P. Mayer Alegre, J. Chan, M. Eichenfield, M. Winger, Q. Lin, J. T. Hill, D. E. Chang, and O. Painter, "Electromagnetically induced transparency and slow light with optomechanics," Nature **472**, 69–73 (2011).
9. C.-H. Dong, V. Fiore, M. C. Kuzyk, and H. Wang, "Transient optomechanically induced transparency in a silica microsphere," Phys. Rev. A **87**, 055802 (2013).
10. E. Verhagen, S. Deléglise, S. Weis, A. Schliesser, and T. J. Kippenberg, "Quantum-coherent coupling of a mechanical oscillator to an optical cavity mode," Nature **482**, 63–67 (2012).
11. G. Anetsberger, O. Arcizet, Q. P. Unterreithmeier, R. Rivière, A. Schliesser, E. M. Weig, J. P. Kotthaus, and T. J. Kippenberg, "Near-field cavity optomechanics with nanomechanical oscillators," Nat. Phys. **5**, 909–914 (2009).
12. G. Anetsberger, E. Gavartin, O. Arcizet, Q. P. Unterreithmeier, E. M. Weig, M. L. Gorodetsky, J. P. Kotthaus, and T. J. Kippenberg, "Measuring nanomechanical motion with an imprecision below the standard quantum limit," Phys. Rev. A **82**, 061804 (2010).
13. E. Gavartin, P. Verlot, and T. J. Kippenberg, "A hybrid on-chip optomechanical transducer for ultrasensitive force measurements," Nat. Nanotechnol. **7**, 509–514 (2012).
14. V. Fiore, Y. Yang, M. C. Kuzyk, R. Barbour, L. Tian, and H. Wang, "Storing optical information as a mechanical excitation in a silica optomechanical resonator," Phys. Rev. Lett. **107**, 133601 (2011).
15. C.-H. Dong, V. Fiore, M. C. Kuzyk, and H. Wang, "Optomechanical dark mode," Science **338**, 1609–1613 (2012).
16. J. T. Hill, A. H. Safavi-Naeini, J. Chan, and O. Painter, "Coherent optical wavelength conversion via cavity optomechanics," Nat. Commun. **3**, 1196 (2012).
17. V. Fiore, C.-H. Dong, M. C. Kuzyk, and H. Wang, "Optomechanical light storage in a silica microresonator," Phys. Rev. A **87**, 023812 (2013).
18. Y.-C. Liu, Y.-F. Xiao, Y.-L. Chen, X.-C. Yu, and Q.-H. Gong, "Parametric down-conversion and polariton pair generation in optomechanical systems," Phys. Rev. Lett. **111**, 083601 (2013).

19. Y.-C. Liu, Y.-F. Xiao, X. Luan, and C.-W. Wong, "Dynamic dissipative cooling of a mechanical resonator in strong coupling optomechanics," Phys. Rev. Lett. **110**, 153606 (2013).
20. C.-H. Dong, V. Fiore, M. C. Kuzyk, L. Tian, and H. Wang, "Optical wavelength conversion via optomechanical coupling in a silica resonator," Annalen der Physik **527**, 100–106 (2015).
21. K. J. Vahala, "Optical microcavities," Nature **424**, 839–846 (2003).
22. M. S. Murib, E. Yüce, O. Gürlü, and A. Serpengüzel, "Polarization behavior of elastic scattering from a silicon microsphere coupled to an optical fiber," Photon. Res. **2**, 45–50 (2014).
23. A. B. Matsko and V. S. Ilchenko, "Optical resonators with whispering-gallery modes-part I: basics," IEEE J. Quantum Electron. **12**, 3–14 (2006).
24. C.-L. Zou, F. J. Shu, F.-W. Sun, Z.-J. Gong, Z.-F. Han, and G.-C. Guo, "Theory of free space coupling to high-*Q* whispering gallery modes," Opt. Express **21**, 9982–9995 (2013).
25. A. J. R. MacDonald, G. G. Popowich, B. D. Hauer, P. H. Kim, A. Fredrick, X. Rojas, P. Doolin, and J. P. Davis, "Optical microscope and tapered fiber coupling apparatus for a dilution refrigerator," Rev. Sci. Instrum. **86**, 013107 (2015).
26. Y.-Z. Yan, C.-L. Zou, S.-B. Yan, F.-W. Sun, Z. Ji, J. Liu, Y.-G. Zhang, L. Wang, C.-Y. Xue, W.-D. Zhang, Z. F. Han, and J.-J. Xiong, "Packaged silica microsphere-taper coupling system for robust thermal sensing application," Opt. Express **19**, 5753–5759 (2011).
27. P.-F. Wang, M. Ding, T. Lee, G. S. Murugan, L. Bo, Y. Swmwnova, Q. Wu, D. Hewak, G. Brambilla, and G. Farrell, "Packaged chalcogenide microsphere resonator with high *Q*-factor," Appl. Phys. Lett. **102**, 131110 (2013).
28. P.-F. Wang, M. Ding, G. S. Murugan, L. Bo, C. Guan, Y. Swmwnova, Q. Wu, G. Farrell, and G. Brambilla, "Packaged, high-*Q*, microsphere-resonator-based add–drop filter," Opt. Lett. **39**, 5208–5211 (2014).
29. F. Vanier, Y.-A. Peter, and M. Rochette, "Cascaded Raman lasing in packaged high quality As_2S_3 microspheres," Opt. Express **22**, 28731–28739 (2014).
30. Y.-C. Dong, K.-Y. Wang, and X.-Y. Jin, "Packaged microsphere-taper coupling system with a high *Q* factor," Appl. Opt. **54**, 277–284 (2015).
31. F. Monifi, S. K. Ozdemir, J. Friedlein, and L. Yang, "Encapsulation of a fiber taper coupled microtoroid resonator in a polymer matrix," IEEE Photon. Technol. Lett. **25**, 1458–1461 (2013).
32. Y.-S. Park, "Radiation pressure cooling of a silica optomechanical resonator," Ph.D. thesis (University of Oregon, 2009).
33. Y. Chen, Z. Shen, C. Dong, C. Zou, and G. Guo, "Mechanical bound state in the continuum for cavity optomechanics" (in preparation).
34. T. Carmon, L. Yang, and K. J. Vahala, "Dynamical thermal behavior and thermal self stability of microcavities," Opt. Express **12**, 4742 (2004).
35. T. J. Kippenberg, S. M. Spillane, and K. J. Vahala, "Kerr-nonlinearity optical parametric oscillation in an ultrahigh-*Q* toroid microcavity," Phys. Rev. Lett. **93**, 083904 (2004).
36. T. J. Kippenberg, H. Rokhsari, T. Carmon, A. Scherer, and K. J. Vahala, "Analysis of radiation-pressure induced mechanical oscillation of an optical microcavity," Phys. Rev. Lett. **95**, 033901 (2005).
37. R. Rivière, O. Arcizet, A. Schliesser, and T. J. Kippenberg, "Evanescent straight tapered-fiber coupling of ultra-high *Q* optomechanical micro-resonators in a low-vibration helium-4 exchange-gas cryostat," Rev. Sci. Instrum. **84**, 043108 (2013).
38. G. Anetsberger, R. Rivière, A. Schliesser, O. Arcizet, and T. J. Kippenberg, "Ultralow-dissipation optomechanical resonators on a chip," Nat. Photonics **2**, 627–633 (2008).
39. J. C. Knight, G. Cheung, F. Jacques, and T. A. Birks, "Phase-matched excitation of whispering-gallery-mode resonances by a fiber taper," Opt. Lett. **22**, 1129–1131 (1997).
40. C.-L. Zou, Y. Yang, C.-H. Dong, Y.-F. Xiao, X.-W. Wu, Z.-F. Han, and G.-C. Guo, "Taper-microsphere coupling with numerical calculation of coupled-mode theory," J. Opt. Soc. Am. B **25**, 1895–1898 (2008).
41. B. E. Little, J. P. Laine, and H. A. Haus, "Analytic theory of coupling from tapered fibers and half-blocks into microsphere resonators," J. Lightwave Technol. **17**, 704–715 (1999).
42. C.-H. Dong, C.-L. Zou, J.-M. Cui, Y. Yang, Z.-F. Han, and G.-C. Guo, "Ringing phenomenon in silica microspheres," Chin. Opt. Lett. **7**, 299–301 (2009).